Allergen-loaded strontium-doped hydroxyapatite spheres improve allergen-specific immunotherapy in mice

Garbani, M ; Xia, W ; Rhyner, C ; Prati, M ; Scheynius, A ; Malissen, B ; Engqvist, H ; Maurer, M ; Crameri, R ; Terhorst, D

Abstract: Background Immunomodulatory interventions play a key role in the treatment of infections and cancer as well as allergic diseases. Adjuvants such as micro- and nanoparticles are often added to immunomodulatory therapies to enhance the triggered immune response. Here, we report the immunological assessment of novel and economically manufactured microparticle adjuvants, namely strontium-doped hydroxyapatite porous spheres (SHAS), which we suggest for the use as adjuvant and carrier in allergen-specific immunotherapy (ASIT). Methods and Results Scanning electron microscopy revealed that the synthesis procedure developed for the production of SHAS results in a highly homogeneous population of spheres. SHAS bound and released proteins such as ovalbumin (OVA) or the major cat allergen Fel d 1. SHAS-OVA were taken up by human monocyte-derived dendritic cells (mdDCs) and murine DCs and did not have any necrotic or apoptotic effects even at high densities. In a murine model of ASIT for allergic asthmatic inflammation we found that OVA released from subcutaneously injected SHAS-OVA led to a sustained stimulation of both CD4+ and CD8+ T-cells. ASIT with SHAS-OVA as compared to soluble OVA resulted in similar humoral responses but in a higher efficacy as assessed by symptom scoring. Conclusion We conclude that SHAS may constitute a suitable carrier and adjuvant for ASIT with great potential due to its unique protein-binding properties.

DOI: https://doi.org/10.1111/all.13041

Received Date : 02-May-2016

Revised Date : 31-Aug-2016

Accepted Date : 01-Sep-2016

Article type : Original Article: Experimental Allergy and Immunology

Editor : Hans-Uwe Simon

Allergen-loaded strontium-doped hydroxyapatite spheres improve allergen-specific immunotherapy in mice

M. Garbani[1], W. Xia[2], C. Rhyner[1], M. Prati[1], A. Scheynius[3], B. Malissen[4], H. Engqvist[2], M. Maurer[5], R. Crameri[1]* & D. Terhorst[4,5,6]

[1]Swiss Institute of Allergy and Asthma Research (SIAF), University of Zurich, Davos Platz, Switzerland

[2]Applied Materials Science, Department of Engineering Sciences, Ångström Laboratory, Uppsala University, Uppsala, Sweden

[3]Department of Clinical Science and Education, Karolinska Institutet, and Sachs' Children and Youth Hospital, Södersjukhuset, 11883 Stockholm, Sweden

[4]Centre d'Immunologie de Marseille-Luminy (CIML), INSERM U1104, CNRS UMR7280, UM2 Aix-Marseille Université, 13288 Marseille Cedex 9, France

[5]Allergie-Centrum-Charité, Department of Dermatology and Allergy, Charité -Universitätsmedizin Berlin, Germany

[6]Berlin Institute of Health (BIH), Berlin, Germany

Short title: Hydroxyapatite spheres in immunotherapy

***Corresponding author:** Prof. Reto Crameri, PhD

Department Molecular Allergology,

Swiss Institute of Allergy and Asthma Research (SIAF), Obere Strasse 22, CH-7270 Davos, Switzerland

Phone: +41 81 410 08 48

FAX: +41 81 410 08 40

Email: crameri@siaf.uzh.ch

Abstract

Background: Immunomodulatory interventions play a key role in the treatment of infections and cancer as well as allergic diseases. Adjuvants such as micro- and nanoparticles are often added to immunomodulatory therapies to enhance the triggered immune response. Here, we report the immunological assessment of novel and economically manufactured microparticle adjuvants, namely strontium-doped hydroxyapatite porous spheres (SHAS), which we suggest for the use as adjuvant and carrier in allergen-specific immunotherapy (ASIT).

Methods and Results: Scanning electron microscopy revealed that the synthesis procedure developed for the production of SHAS results in a highly homogeneous population of spheres. SHAS bound and released proteins such as ovalbumin (OVA) or the major cat allergen Fel d 1. SHAS-OVA were taken up by human monocyte-derived dendritic cells (mdDCs) and murine DCs and did not have any necrotic or apoptotic effects even at high densities. In a murine model of ASIT for allergic asthmatic inflammation we found that OVA released from subcutaneously injected SHAS-OVA led to

a sustained stimulation of both $CD4^+$ and $CD8^+$ T-cells. ASIT with SHAS-OVA as compared to soluble OVA resulted in similar humoral responses but in a higher efficacy as assessed by symptom scoring.

Conclusion: We conclude that SHAS may constitute a suitable carrier and adjuvant for ASIT with great potential due to its unique protein-binding properties.

Keywords: allergy model, dendritic cells, immunotherapy, microparticles

Introduction

The mechanisms by which micro- and nanoparticles enhance immune responses to antigens are diverse and include the delivery of antigens and the direct stimulation of the immune cells, as recently reviewed (1). The administration of an antigen in a particulate form has been postulated to enhance its stability and integrity and to create a so-called depot effect, where the antigen is gradually released, thus prolonging the challenge of the immune system (2).

Allergen-specific immunotherapy (ASIT) is used as a desensitizing therapy for allergic diseases and is a specific and potentially curative treatment. The mechanisms of action of ASIT include the modulation of T- and B-cell responses and related antibody isotypes, as well as the regulation of eosinophils, basophils and mast cells in terms of migration to the tissues and release of mediators (3). Dendritic cells (DCs) as primer of the adaptive immune response are key cells for a successful ASIT. Recent research identified several subsets of DCs equipped with different functional properties, ranging from tolerance-induction to the promotion of specific immune responses (4). Subcutaneous immunotherapy protocols generally involve daily to weekly injections during a build-up phase, followed by monthly maintenance injections for a period of 3–5 years (5). A prolonged presence of the antigen is needed for the induction of tolerance. Current ASIT protocols are time-consuming which leads to a low compliance of patients. Better therapeutic options are needed to meet this medical need.

The strontium-doped hydroxyapatite porous spheres (SHAS) used in this study are the result of an optimized synthesis procedure that allows for controlling their size, porosity and morphology (6). Similar spheres, hollow calcium phosphate spheres, have been shown to bind consistent amounts (~0.37 mg/mg) of the antibiotics vancomycin and cephalothin, which are then slowly released over many hours *in vitro* (7). In this study, we evaluated the potential of SHAS as a matrix for a prolonged local delivery of protein antigen, and we assessed their potential as a tolerance-inducing adjuvant for immunotherapeutic interventions, specifically ASIT.

Material and Methods

Preparation and characterization of SHAS, strontium-doped hydroxyapatite porous spheres

NaCl, KCl, Na_2HPO_4, and KH_2PO_4 were dissolved in sterile water at a molar ratio of 137.0 : 2.7 : 8.1 : 1.5 : 0.5. After addition of calcium chloride (1 mM), magnesium chloride (0.05 mM) and strontium nitrate (0.6 mM), the mixture was heated at 100°C. After 6 hours, the precipitation was filtered and washed twice with room-temperature ethanol. All chemicals were purchased from Sigma-Aldrich (Steinheim, Germany) at the highest purity grade available. The morphology of the spheres before and after OVA adsorption was analyzed by Field Emission Scanning Electron Microscopy (FE-SEM, LEO 1550, Zeiss, Germany). Powder X-ray diffraction (XRD, Siemens Diffractometer D5000, Siemens, Munich, Germany) using Cu Kα radiation (λ = 1.5418 Å) operated at 40 kV and 40 mA at a 2θ range of 5° - 60°C was used to analyze the crystallinity of SHAS. Surface area and porosity were estimated from the N_2 sorption isotherm, which was performed by Accelerated Surface Area and Porosimetry (ASAP 2020, Micromeritics, Norcross, GA, United States) in accordance with the Brunauer-Emmet-Teller principle. The ion composition was analyzed using inductive coupled plasma optical emission spectroscopy (ICP-OES, Optima 5300DV; Perkin-Elmer, Waltham, MA, United States). The zeta-potential of the particles was measured in PBS at 25°C and 37°C by laser Doppler velocimetry on a

ZetaSizer Nano instrument (Malvern Instruments, UK). The refraction indexes used were of 1.63 for the particles. LPS contamination was ruled out indirectly measuring NF-κB activation in human mdDCs (data not shown).

Ovalbumin labeling

Grade VI OVA (Sigma-Aldrich) and Dylight 488 Amine-Reactive Dye (Thermo Scientific, Rockford, IL, United States) were used to produce labeled OVA_{488}. To this end, OVA was suspended in phosphate buffered saline (PBS) at a concentration of 2 mg/ml, sterilized by filtration and added to the vial containing the dye. After 3 h incubation at room temperature and 12 h at 4°C, the unreacted dye was removed by dialysis against PBS with a SpectraPor Membrane with a molecular weight cut-off of 6-8 kDa (Spectrum Labs, Roncho Domingues, CA, United States) and 4 buffer exchanges over 36 h.

Protein loading of SHAS

SHAS (1-5 mg) were suspended in 500 µl PBS and put in a sonication bath five times for 10 s in order to obtain a homogeneous solution. Between each sonication burst the tubes were shaken by hand. The SHAS were allowed to stand for 5 min, centrifuged (2000 x g, 2 min), and washed once with 500 µl PBS. Afterwards they were suspended in 300 µl of 1 mg/ml protein solution per mg of particles and left overnight under constant shaking. Thereafter, the beads were collected by centrifugation (2000 x g, 2 min) and the protein concentration in the supernatant was determined by Bradford (Biorad, Hercules, CA, United States) to calculate the amount of protein loaded. The major cat allergen Fel d 1, used as a protein loading control for SHAS, was produced in *E. coli* and purified as described (8). LPS decontamination was ruled out indirectly measuring NF-κB activation in human mdDCs (data not shown).

In vitro release

Two mg of OVA_{488}-loaded SHAS were suspended in 200 µl PBS or PBS-Tween20 (0.05%) and kept in suspension by rolling at room temperature. Spontaneous release was monitored by measuring the protein concentration in the supernatant after 20 h. The quality of the protein released was visualized by sodium dodecyl sulphate-polyacrylamide gel electrophoresis (SDS-PAGE). Residual protein bound to the SHAS was released by incubation for 5 min at 90°C in SDS-PAGE loading buffer (50 mM Trizma-HCl pH8, 5% glycerol, 2.5% β-mercaptoethanol, 50 µg/ml bromophenol blue, 10% dithiothreitol, all from Sigma-Aldrich).

Preparation of monocyte-derived dendritic cells (mdDCs)

Human mdDCs were prepared from peripheral blood mononuclear cells from healthy donors with written informed consent. The $CD14^+$ population was isolated by AutoMACS using CD14 microbeads (Miltenyi Biotec, Bergisch Gladbach, Germany) and cultured at 10^6/ml in 6-well plates in cRPMI (RPMI 1640, 10% heat-inactivated FCS, 2 mM L-glutamine, 1 mM sodium pyruvate, 1x MEM vitamins, 1x MEM non-essential amino acids, 100 U/ml penicillin, 100 µg/ml streptomycin, 100 µg/ml kanamycin, all from Sigma-Aldrich) in the presence of 1000 U/ml GM-CSF (PeproTech, Hamburg, Germany) and 1000 U/ml IL-4 (Novartis, Basel, Switzerland) for 5 days. The successful differentiation to human mdDCs was confirmed by flow cytometric CD11c staining (clone 3.9, Biolegend, Biolegend, San Diego, USA) together with the viability staining agent eFluor 780 (eBioscience, Vienna, Austria, data not shown). Cells were stained and analyzed using a FACS LSRII or a Canto system with DIVA software (BD Biosciences).

In vitro toxicity, apoptosis detection assays

100, 10, or 1 μg of SHAS were added to 2 x 10^5 human mdDCs in 200 μl cRPMI in a 96-well plate. After 24 h incubation, the cells were stained for Annexin and 7AAD with the PE Annexin V Apoptosis Detection Kit I (BD Biosciences, Erembodegen-Aalst, Belgium) and analyzed by flow cytometry.

Mice

7-10 weeks old female B6 wild type, C57BL/6 or BALB/c mice were housed under specific pathogen free (SPF) conditions and handled in accordance with French and European directives with ethical approval from the Centre d'Immunologie de Marseille-Luminy. OT-I and OT-II mice have been previously described (9, 10).

Sensitization and immunotherapy models

The models are described in Fig. S1.

Preparation and adoptive transfer of labeled OT-I and OT-II cells

OVA-specific $CD8^+$ (OT-I) and OVA-specific $CD4^+$ (OT-II) T-cells were isolated as previously described (11), labeled with CellTrace Violet (CTV, Invitrogen), adoptively transferred and after 3 days isolated from the spleen and analyzed by flow cytometry (see Fig. S1A).

Flow cytometry of mouse cells

Single cell suspension of lymph nodes were produced as previously described (11). Cells were stained and analyzed using a FACS LSRII or a Canto system with DIVA software (BD Biosciences). Cell viability was evaluated using Sytox (Invitrogen Detection Technologies, Eugene, USA).

Anti-CD3 (17A2) was from Biolegend (San Diego, USA), TCR Vα2 (6D6.6) from Abcam, anti-CD45.1 (A20) from eBioscience, anti-CD4 (RM4-5), and anti-CD8α (53-6.7) were from BD Pharmingen (San Diego, USA).

For the analysis of the nodal DCs the following antibodies were additionally used: anti-NK1.1 (PK136), anti-CD19 (6D5), anti–Ly-6G (1A8) and anti-CD64 (X54-5/7.1) from BioLegend; anti-CD11b (M1/70), anti-CD11c (N418), anti–MHC class II (MHC II; I-A/I-E) (M5/114.15.2) and anti-CD24 (M1/69) from eBioscience.

Analyses were performed on living $CD45^+$ cells. Prior to analyzing DCs, we systematically gated out B cells, T cells, NK cells, macrophages and neutrophils using a dump channel corresponding to cells positive for CD19, CD3, NK1.1, CD64 or Ly-6G cells. The migratory DCs were characterized as $MHC\text{-}II^{high}$ and $CD11c^{low\text{-}high}$. We further discriminated migratory DCs into $CD11b^+CD24^-$ and $CD24^+$ cells.

Analysis was performed using FlowJo software (Tree Star, Inc., Ashland, OR, USA).

Microscopy

Fluorescent OVA (OVA_{488}) labeled SHAS (prepared as described above) were added to 300'000 mdDCs at a concentration of 25 μg/ml in cRPMI. After 12 h the cells were washed once with PBS and resuspended in 200 μl PBS at 37°C. CellMask Orange Plasma membrane Stain (Thermo Scientific) was diluted 1:5000 in PBS, vortexed for 30 s and sonicated for 1 min. After warming at 37°C for 3 min in a water bath 100 μl of this solution was added to the mdDCs and incubated by rolling for 10 min at room temperature. Stained cells were washed twice with PBS and brought onto a microscope slide by cytospin (500 rpm, 2 min), fixed with 4% paraformaldehyde (Sigma-Aldrich), covered with Prolong Gold Antifade Reagent with DAPI (Life Technologies) and visualized by a Leica TCS SPE confocal microscope (Leica Microsystems, Heerbrugg, Switzerland).

Immunoglobulin ELISA

Nunc-Immuno Clear Flat-Bottom Maxisorp 96-well plates (Thermo Scientific) were coated by overnight incubation at 4°C with 100 µl of 10 µg/ml OVA in PBS. Unspecific bindings were avoided by 1 h incubation in 150 µl blocking buffer (1% BSA and 5% sucrose in PBS, all from Sigma-Aldrich). After washing, 100 µl diluted sera (1:10 for IgE, 1:100 for IgG_{2a}, 1:100'000 for IgG_1) were added and incubated for 3 h. OVA-specific antibodies were detected with 100 µl of the corresponding biotinylated anti-isotype at 0.5 µg/ml and incubated for 2 h. After 45 min incubation with Streptavidin-HRP diluted 1:200 (R&D Systems, Minneapolis, MN, United States), bound antibodies were detected with OptiEIA TMB Substrate Reagent (BD Biosciences). Antibodies, sera and enzymes were diluted in PBS containing 1% BSA. Between each step, plates were washed 3 times with PBS-Tween (0.05%). The following anti-isotype antibodies were used: biotin anti-mouse IgE (RME-1), biotin anti-mouse IgG_1 (RMG1-1), and biotin anti-mouse IgG_{2a} (RMG2a-62; all from Biolegend). Serum concentrations were calculated by 4-parametric curve regression using the following antibodies as standards (50-0.4 ng/ml): mouse anti-OVA IgE (2C6; AbD Serotec, Raleigh, NC, USA), mouse anti-denatured OVA IgG_1 and mouse anti-denatured OVA IgG_{2a} (6C8, 6G2; Thermo Scientific).

Bronchoalveolar lavage

Mice were sacrificed by intraperitoneally injection of pentobarbital (150 mg/kg, Streuli Pharma AG, Uznach, Switzerland). Broncho alveolar lavage (BAL) was performed by sealing the upper part of the trachea with medical tweezers and injecting 1 ml PBS containing the cOmplete proteinase inhibitor cocktail (Roche, Mannhein, Germany), using a 1 ml syringe with a bent 26G needle. Determination of cell type and content in BAL was determined by Romanowski stain (Diff-Quick, Medion Diagnostics, Düdingen, Switzerland) for cell subsets.

Behavioral assessments

To assess pain or discomfort, mice were observed in an open-field test. After immunotherapeutic injections every mouse was allowed to rest for 45 min in the home cage. Afterwards it was transferred to a 30x50 cm cage divided into 10x10 cm squares and observed for 3 min. The following parameters were recorded and scored as follows: fur (1 point if crumpled, 2 points if very sweaty), posture (1 point if the mouse was crooked, 2 points for no locomotion), movement (full body access to the 10 cm sectors, 1 point for only entering 4-10 sectors, 2 points for only entering 1-3 sectors), rearing behavior (1 point if absent), urination and defecation (1 point if absent). The cage was cleaned first with a humid cloth and then with a dry one before starting the experiment with another animal (adapted from (12, 13).

Statistical analysis

The Wilcoxon-Mann-Whitney-Test was used to assess statistical significance. Probability values are expressed as the following: ***, $p<0.001$; **, $p<0.01$; *, $p<0.05$; NS, non significant.

Results

Physical characterization of SHAS

The synthesis procedure developed for the production of SHAS resulted in a homogeneous population of spheres as assessed by scanning electron microscopy (Fig. 1A). The molar ratio of their composition was 1.00 (Magnesium) : 2.15 (Strontium) : 3.85 (Calcium) : 5.42 (Phosphate). SHAS mainly consisted of hydroxyapatite as shown by X-ray diffraction analysis, where peaks were coherent with the joint committee on powder diffraction standards (JCPDS) data (JCPDS-09-

0432/1996, Fig. 1B). The zeta-potential of SHAS in PBS resulted in a negative value of -10.5 ± 1.3 mv (mean ±SEM, n>3) at 25° C and of -12.1 ± 4.0 mv at 37° C.

The spheres exhibited a spherical and porous shape. Scanning electron microscopy showed an average diameter of 1.8 μm, with a range of 1.3 – 2.5 μm. The pore size of 33.1 nm in spheres was obtained from BET analysis (Fig. 1C). One mg of SHAS bound approximately 90 μg of both the model antigen OVA and the control protein Fel d 1, the major cat allergen (Fig. 1D). OVA binding did not influence the morphology of SHAS as demonstrated by electron microscopy (Fig. 1C), and the particle-bound OVA did not appear degraded or modified after spontaneous or Tween20-induced release (Fig. 1E).

OVA-loaded SHAS is taken up by human mdDCs without toxic and apoptosis inducing side effects in vitro

In order to test the compatibility and properties of SHAS on human antigen-presenting cells we added the particles to mdDCs. DyLight$_{488}$ labelled OVA (OVA$_{488}$), previously loaded on SHAS (SHAS-OVA$_{488}$), was taken up and internalized by human mdDCs after 1 h incubation (Fig. 2A). No difference in toxicity or apoptosis induction compared to untreated human mdDCs was seen when different concentrations of soluble OVA$_{488}$, SHAS- OVA$_{488}$ or SHAS alone were added to the cells (Fig. 2B).

Uptake of antigens by DCs in vivo

To quantify the uptake of antigens *in vivo*, we injected either soluble OVA labeled with DyLight$_{488}$ (OVA$_{488}$), OVA$_{488}$ bound to microparticles (SHAS-OVA$_{488}$), or PBS subcutaneously into the lumbar area of B6-WT mice which were sacrificed 1, 4 or 7 day(s) after injection. Then we analyzed the migrated DCs in the draining inguinal lymph nodes for their uptake of OVA$_{488}$ by flow cytometry.

DyLight$_{488}^{+}$ cells were detectable among migratory DCs 1 day after injection of both OVA$_{488}$ and of SHAS-OVA$_{488}$ (Fig. 2C). We further discriminated DCs cells into CD11b^{+}CD24^{-} and CD24^{+} cells and among the CD11b^{+}CD24^{+} DCs we see a small but consistent uptake of OVA$_{488}$ bound to SHAS, which persisted for the total period of investigation of 7 days (Fig. 2D).

SHAS-OVA induces a stronger OVA-specific CD4^{+} and CD8^{+} T- cell proliferation compared to OVA

To test whether targeting DCs with antigen-loaded SHAS can induce the activation of antigen-specific T cells *in vivo*, we injected SHAS-OVA or soluble OVA subcutaneously in mice. After 3, 6 or 8 days, mice were adoptively transferred with CTV labeled OT-I CD8^{+} T cells and OT-II CD4^{+} T cells. They express a TCR specific for an OVA-derived peptide presented by H-2Kb and for an OVA-derived peptide presented by H2-Ab, respectively (9, 10). Three days after adoptive transfer, the extent of OT-I and OT-II cell proliferation was determined by CTV dilution (Fig. S1A). SHAS-OVA triggered a significantly higher proliferation of OT-I and OT-II cells than soluble OVA (Fig. 3A, B). Furthermore, SHAS-OVA, but not soluble OVA, resulted in sustained T cell proliferation for up to 6 and 8 days in CD4^{+} and CD8^{+} T cells, respectively.

OVA-specific IgE and IgG responses to SHAS-bound OVA are comparable to those obtained with soluble OVA

Next, we wanted to investigate the induction of antigen specific IgE and IgG production in response to SHAS-OVA compared to soluble OVA. To do so, we used a standard protocol for sensitization to allergens consisting of a sensitization period with three weekly injections of SHAS-OVA or the adequate amount of OVA as well as injections with Alum-OVA, PBS and SHAS alone as controls. Following the sensitization period, the challenge consisted of three injections of OVA at days 26, 27 and 28 (Fig. S1B).

Humoral responses, in particular serum levels of antigen-specific IgE, IgG_1 and IgG_{2a}, were comparable in mice immunized with SHAS-OVA and soluble OVA. (Fig. 4A-C). Moreover, following aerosol allergen challenge, the amount of eosinophils in the BAL fluid was comparable for sensitization with OVA, SHAS-OVA and Alum-OVA, indicating analogous levels of allergic sensitization (Fig. 4D).

SHAS immunotherapy has increased efficacy

To assess the potential of SHAS as an antigen-carrier for immunotherapeutic interventions for allergic diseases, we used a rush immunotherapy protocol consisting of a sensitization period followed by treatment with OVA, SHAS-OVA or protein-free SHAS. As control, we also added a group of mice (OVA-ctrl) treated more frequently and with a higher dose of OVA (14). After the treatment, mice were challenged with OVA (Fig. S1C). Behavioral assessments evaluated pain and discomfort using a symptom score as described in the material and methods section. Immunotherapy using SHAS-OVA showed a stronger reduction of the symptoms assessed following both the first and the last immunotherapeutic injection than did soluble OVA or SHAS alone (Fig. 5A, B). Regarding the other parameters assessed, such as eosinophils in BAL and antigen specific IgG_1, no difference was seen between the groups treated with SHAS-OVA, soluble OVA or SHAS alone (Fig. 5C, D).

Discussion

ASIT is a safe and effective treatment for type I respiratory allergies in humans. Better adjuvants could further improve ASIT, allowing to decrease the allergen dose and to simplify immunization schemes. The present study showed that the use of SHAS, strontium-doped hydroxyapatite spheres, in ASIT can help to target the allergen to DCs and thereby enhance ASIT efficacy. Specifically, SHAS can bind allergens, facilitate allergen-specific immune response and improve the clinical outcome of ASIT.

The loading of SHAS with the model allergen OVA enhances OVA stability and integrity, creates sustained release and depot effects, and results in sustained immune responses after application *in vivo*. One single subcutaneous injection of the antigen-loaded particles was sufficient to induce antigen-specific $CD8^+$ and $CD4^+$ effector T cells over at least 6 days. Allergens loaded on SHAS are taken up by dendritic cells and the microparticles do not have toxic or apoptosis-inducing effects. Importantly, in a mouse model of ASIT, SHAS-OVA led to a better symptom reduction compared to OVA alone. OVA_{488} released from SHAS-OVA_{488} was mostly taken up by $CD11b^+$ DCs. This DC subset constitutively produces retinoic acid and induces Foxp3+ regulatory T cells (15). Targeting of this tolerogenic $CD11b^+$ DC subset could thus be one possible explanation for the successful ASIT using SHAS-bound proteins.

A main advantage of the use of allergen-delivery systems in immunotherapy is that the antigen release is continuous, which could make single shot treatments as effective as the currently employed and less convenient multiple dosage protocols (16, 17). Biodegradable nanoparticles such as SHAS encapsulate allergens so that they are delivered *in vivo* in a delayed-continuous or pulsatile manner to modulate the resultant immune response and decrease the potential for adverse events (18). Our study supports this hypothesis as the injection with the slowly and continuously released OVA bound to SHAS resulted in a better response compared to the injection of the soluble, directly available OVA.

We have previously shown that the production of SHAS is straightforward, relatively inexpensive and robust (6). SHAS have been hitherto used as biomaterial for bone reconstruction, and now for the first time they are used in the field of immunology (19, 20). Here, we show that ASIT with SHAS-bound allergen is more effective than immunotherapy with soluble allergen. Taken together, these findings recommend further development of SHAS for the use in allergen-specific immunotherapy.

Acknowledgement

This study was supported by ERA-Net EuroNanoMed, NANOASIT I (Novel drug delivery routes mediated via nanotechnology; targeting allergy vaccination), ERA-Net EuroNanoMed2 NANOASIT II (Allergy vaccination using novel drug delivery routes mediated via nanotechnology), and the Swedish Research Council (to A.S. and 2013-5419 to W.X. and H.E.). Dr. Terhorst is participant in the BIH-Charité Clinical Scientist Program funded by the Charité –Universitätsmedizin Berlin and the Berlin Institute of Health.

Conflict of interest

The authors declare no conflict of interest.

Author contributions

This study was conducted in the frame of NANOASIT I and NANOASIR II. All authors had a part in the study design and conduction of the study, had full access to the data, actively participated to the interpretation of the data, writing of the manuscript, and gave final approval for publication. W.X. and H.E. provided the microparticles, M.G. performed most of the experiments, D.T. prepared the manuscript.

References

1. Smith DM, Simon JK, Baker JR, Jr. Applications of nanotechnology for immunology. *Nat Rev Immunol* 2013;**13**(8):592-605.

2. Henriksen-Lacey M, Christensen D, Bramwell VW, Lindenstrom T, Agger EM, Andersen P, et al. Liposomal cationic charge and antigen adsorption are important properties for the efficient deposition of antigen at the injection site and ability of the vaccine to induce a CMI response. *J Control Release* 2010;**145**(2):102-108.

3. Akdis CA, Akdis M. Mechanisms of allergen-specific immunotherapy. *J Allergy Clin Immunol* 2011;**127**(1):18-27; quiz 28-19.

4. Malissen B, Tamoutounour S, Henri S. The origins and functions of dendritic cells and macrophages in the skin. *Nat Rev Immunol* 2014;**14**(6):417-428.

5. Jutel M, Agache I, Bonini S, Burks AW, Calderon M, Canonica W, et al. International consensus on allergy immunotherapy. *J Allergy Clin Immunol* 2015;**136**(3):556-568.

6. Xia W, Grandfield K, Schwenke A, Engqvist H. Synthesis and release of trace elements from hollow and porous hydroxyapatite spheres. *Nanotechnology* 2011;**22**(30):305610.

7. Xia W, Mojo MZ, Persson C, Engqvist H. Self-assembled hollow hydroxyapatite spheres for ion and drug delivery. In: Proceedings of the 12th Conference of the European Ceramic Society - EcerS XII; 2011; Stockolm, Sweden; 2011.

8. Gronlund H, Bergman T, Sandstrom K, Alvelius G, Reininger R, Verdino P, et al. Formation of disulfide bonds and homodimers of the major cat allergen Fel d 1 equivalent to the natural allergen by expression in Escherichia coli. *J Biol Chem* 2003;**278**(41):40144-40151.

9. Barnden MJ, Allison J, Heath WR, Carbone FR. Defective TCR expression in transgenic mice constructed using cDNA-based alpha- and beta-chain genes under the control of heterologous regulatory elements. *Immunol Cell Biol* 1998;**76**(1):34-40.

10. Hogquist KA, Jameson SC, Heath WR, Howard JL, Bevan MJ, Carbone FR. T cell receptor antagonist peptides induce positive selection. *Cell* 1994;**76**(1):17-27.

11. Terhorst D, Fossum E, Baranska A, Tamoutounour S, Malosse C, Garbani M, et al. Laser-assisted intradermal delivery of adjuvant-free vaccines targeting XCR1+ dendritic cells induces potent antitumoral responses. *J Immunol* 2015;**194**(12):5895-5902.

12. Conrad ML, Yildirim AO, Sonar SS, Kilic A, Sudowe S, Lunow M, et al. Comparison of adjuvant and adjuvant-free murine experimental asthma models. *Clin Exp Allergy* 2009;**39**(8):1246-1254.

13. Deacon RM. Housing, husbandry and handling of rodents for behavioral experiments. *Nat Protoc* 2006;**1**(2):936-946.

14. Vissers JL, van Esch BC, Hofman GA, Kapsenberg ML, Weller FR, van Oosterhout AJ. Allergen immunotherapy induces a suppressive memory response mediated by IL-10 in a mouse asthma model. *J Allergy Clin Immunol* 2004;**113**(6):1204-1210.

15. Guilliams M, Crozat K, Henri S, Tamoutounour S, Grenot P, Devilard E, et al. Skin-draining lymph nodes contain dermis-derived CD103(-) dendritic cells that constitutively produce retinoic acid and induce Foxp3(+) regulatory T cells. *Blood* 2010;**115**(10):1958-1968.

16. Uchida T, Martin S, Foster TP, Wardley RC, Grimm S. Dose and load studies for subcutaneous and oral delivery of poly(lactide-co-glycolide) microspheres containing ovalbumin. *Pharm Res* 1994;**11**(7):1009-1015.

17. Slobbe L, Medlicott N, Lockhart E, Davies N, Tucker I, Razzak M, et al. A prolonged immune response to antigen delivered in poly (epsilon-caprolactone) microparticles. *Immunol Cell Biol* 2003;**81**(3):185-191.

18. Sah H, Chien YW. Prolonged immune response evoked by a single subcutaneous injection of microcapsules having a monophasic antigen release. *J Pharm Pharmacol* 1996;**48**(1):32-36.

19. Hulsart-Billstrom G, Xia W, Pankotai E, Weszl M, Carlsson E, Forster-Horvath C, et al. Osteogenic potential of Sr-doped calcium phosphate hollow spheres in vitro and in vivo. *J Biomed Mater Res A* 2013;**101**(8):2322-2331.

20. Cardemil C, Elgali I, Xia W, Emanuelsson L, Norlindh B, Omar O, et al. Strontium-doped calcium phosphate and hydroxyapatite granules promote different inflammatory and bone remodelling responses in normal and ovariectomised rats. *PLoS One* 2013;**8**(12):e84932.

21. Lewis VJ, Thacker WL, Mitchell SH, Baer GM. A new technic for obtaining blood from mice. *Lab Anim Sci* 1976;**26**(2 Pt l):211-213.

Figure Legends

Fig. 1 Characterization of SHAS and their protein binding properties

A) The population of beads as result of the synthesis procedure developed for the creation of SHAS. B) X-Ray diffraction pattern of SHAS and hydroxyapatite. C) Representative SEM images of SHAS before (left) and after OVA binding (right). D) Binding of OVA and the major cat allergen Fel d 1 to SHAS, determined by subtracting the amount of unbound protein in the supernatant after the adsorption process from the initial amount. Results are expressed in µg of protein that bound to 1 mg of SHAS (n=3, mean ± SEM). E) SDS-PAGE before and after binding to SHAS. Line 1, OVA; line 2, PBS-Tween20 released OVA; line 3, PBS released OVA.

Fig. 2 OVA_{488}-loaded SHAS is taken up by human and murine DCs without toxic and apoptotic side effects

A) Human mdDCs after 1 h of incubation with SHAS-OVA_{488} (green: OVA_{488}; white: plasma membrane staining (Cellmask Orange); blue: DAPI); two representative pictures taken by confocal microscopy.

B) Percent of necrotic and apoptotic human mdDCs after 24 h contact with different concentrations of OVA_{488}, SHAS or SHAS-OVA_{488} as determined by 7AAD and anti-annexin staining by flow cytometry (representative plots, n=3).

C) Flow cytometry analysis of the uptake of OVA_{488} by migratory DCs migrated to the draining inguinal lymph node of B6-WT mice 1 day after injection of either PBS, soluble OVA_{488} or SHAS-OVA_{488} into the lumbar area of the mice (representative plots, n=2-3).

D) Percentage of $CD11b^+$ migratory DCs in the draining inguinal lymph node of B6-WT mice which have taken up OVA_{488} ($DyLight488^+$), 1, 4 or 7 days after injection of soluble OVA_{488} or SHAS-OVA_{488} into the lumbar area of the mice (representative plots, n=2-3).

Fig. 3 SHAS-OVA induces a stronger OVA-specific $CD8^+$ (OT-I) and $CD4^+$ (OT-II) T- cell proliferation compared to OVA.

CellTraceViolet (CTV)- labeled OVA-specific $CD8^+$ (OT-I) and $CD4^+$ (OT-II) T cells were adoptively transferred in WT C57/BL6 mice 3, 6 or 8 days after the s.c. injection of OVA_{488} or SHAS-OVA_{488}. The proliferation was assessed in the spleen 3 days later by flow cytometry. After gating on $CD45.1^+$ $CD3^+$ $TCRV\alpha2^+$ $CD8^+$ or $CD4^+$ cells, proliferation was assessed by the dilution of CTV. For experimental protocol see Fig. 6A. Percentage of proliferating OT-I (A) and OT-II T cells (B) is depicted. Significant differences among the groups are marked (*, $p < 0.05$; ***, $p < 0.001$; Two-tailed Mann-Whitney test). Each group consisted of 4 animals.

Fig. 4 OVA-specific IgE and IgG responses to SHAS-bound OVA are comparable to those obtained with soluble OVA.

BALB/c mice were sensitized s.c. with PBS, OVA, SHAS-OVA or SHAS, or i.p with Alum-OVA. The appearance of immunoglobulins in serum was monitored, as well as the number of eosinophils in BAL after OVA challenge as an indicator of inflammation. For experimental protocol see Fig. S1B. A-C Immunoglobulin levels 26 days after the first injection. D) Percentage of eosinophils in BAL fluid after OVA challenge. Different capital letters indicate significant differences among the groups ($p < 0.05$, Two-tailed Mann-Whitney test). OVA and SHAS-OVA treated groups consisted of 5 animals, except for the SHAS-OVA group in panel D which consisted of 4 animals; PBS, SHAS and Alum-OVA treated groups consisted of 4 animals.

Fig. 5 SHAS immunotherapy has reduced side effects.

After sensitization with Alum adsorbed OVA, mice were treated with two s.c. injections of OVA, SHAS or SHAS-OVA (0.2 mg OVA) on days 21 and 28. As a control, higher amounts were injected three times every second day (OVA-Ctrl). Serum samples were collected throughout the experiment as well as the BAL fluid after sacrifice. For experimental protocol see Fig. S1C. A) Symptoms score 45 min after the first immunotherapeutic injection (day 21). B) Symptoms score 45 min after the last immunotherapeutic injection (day 23 for the OVA-Ctrl group, day 28 for the other groups). C) Absolute number of eosinophils in BAL fluid after OVA sensitization, immunotherapy and aerosol challenge (day 40). D) Serum concentration of IgG_1 before the challenge, i.e. at the end of immunotherapy phase (day 35). Significant differences among the groups are marked (*, $p < 0.05$; **, $p < 0.01$; Two-tailed Mann-Whitney test). Each group consisted of 6 animals, except for the SHAS control group, which consisted of 4 animals.

Fig. S1 Immunisation protocols for the data shown in Fig. 3 (A), Fig. 4 (B) and Fig. 5 (C).

A) T cell immune response *in vivo*: C57BL/6 mice were injected s.c. in the lumbar area with 200 µl of a solution containing 20 µg OVA, bound or not bound to SHAS. After 3, 6 or 8 days, 10^6 of both CTV labeled OT-I and OT-II cells were injected i.v. Three days later, splenocytes were isolated and analyzed by flow cytometry.

B) Humoral immune response *in vivo*: To characterize the immune responses to antigens delivered through SHAS, wild-type BALB/c mice were sensitized using an adjuvant-free protocol as described (12), with 3 s.c. injections of 10 µg OVA in solution or bound to SHAS on days 0, 7 and 14. Negative control mice were injected with the corresponding amounts of SHAS or PBS and a positive control group of mice was injected i.p. with 10 µg OVA absorbed to 500 µg Alum (Imject Alum, Thermo

Scientific). Mice were challenged on days 26, 27, 28 with 1% OVA aerosols for 20 min and sacrificed on day 30. Blood samples were taken with the tail cut method (21) on days 0, 14, 26 and 30 and the concentration of OVA-specific IgE, IgG_1 and IgG_{2a} was determined by ELISA. Mice were sacrificed on day 30 and BAL was obtained.

C) Immunotherapy model: The possibility of using SHAS for immunotherapeutic purposes was investigated using a previously described allergy model (14). Wild-type BALB/c mice were sensitized with two i.p. injections of 10 μg OVA precipitated together with 2.25 mg Alum on days 0 and 7. Mice were then treated with two s.c. injections of 0.2 mg OVA, SHAS-OVA or protein-free SHAS on day 21 and 28. On days 21 and 28 (or day 23 for the OVA-Ctrl group), a symptom score was determined. The control immunotherapy group (OVA-ctrl) was treated with three s.c. injections of 1 mg OVA on days 21, 23, 25 (14). On days 35, 37 and 39 mice were challenged with 1% OVA aerosols for 20 min and sacrificed on day 40 and BAL was obtained.

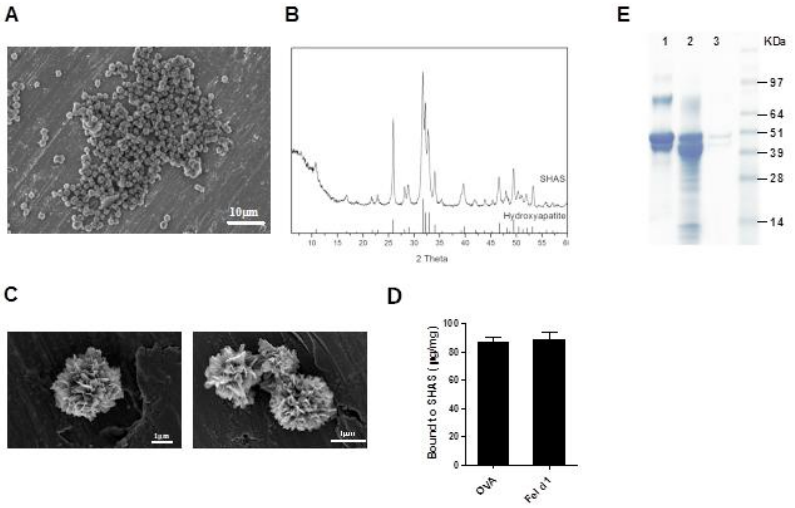

Figure 1

Figure 2

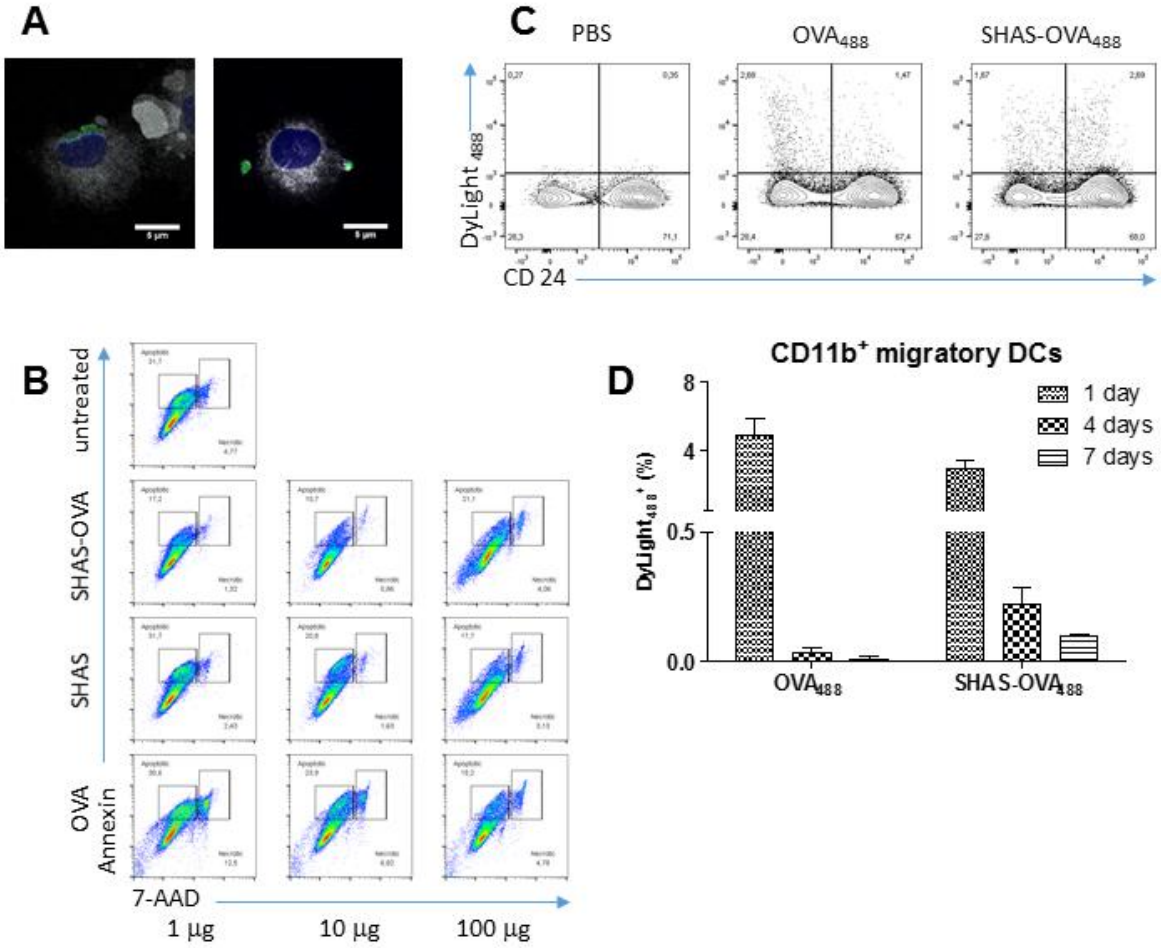

Figure 3

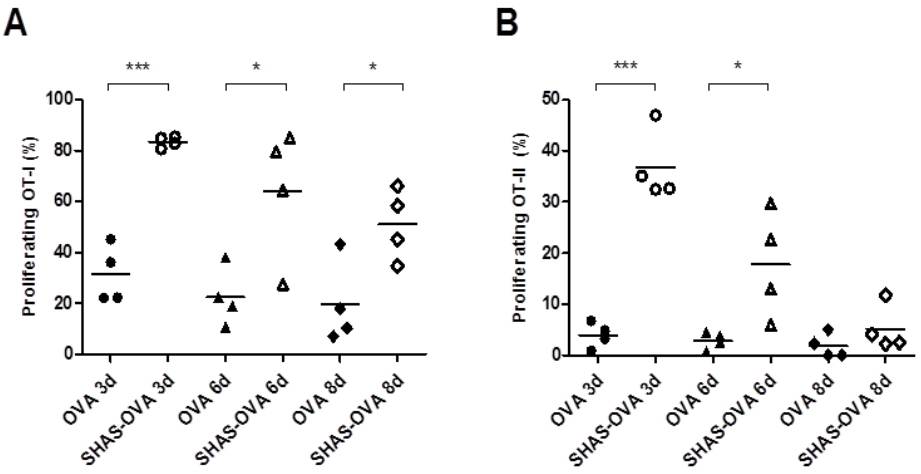

Figure 4

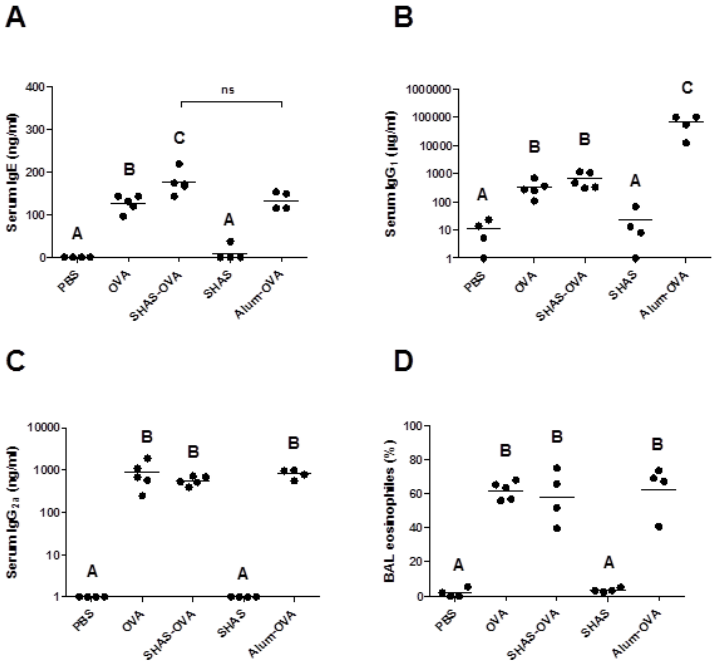

Figure 5